Study of rotation of ellipsoidal particles in combined simple shear flow and magnetic fields

Jie Zhang[1], Cheng Wang[1]
1. Department of Mechanical and Aerospace Engineering, Missouri University of Science and Technology, Rolla, MO, USA

Abstract: Jeffery's theory describes the periodic rotation of ellipsoidal particles in a simple shear flow at vanishing Reynolds number limit. In this paper, we present direct numerical simulations, implemented by using the arbitrary Lagrangian-Eulerian (ALE) method, to study the motion of ellipsoidal paramagnetic particles in a simple shear flow subjected to a uniform magnetic field. We investigated the effect of several parameters, including magnetic field strength, direction of magnetic field, and particle aspect ratio, on rotation period and asymmetry of particle rotation. Without a magnetic field, the simulation results are in good agreement with Jeffery's theory. When a magnetic field is applied perpendicular to the flow direction, the rotational period became longer, and the magnetic field breaks the symmetry of rotational motion of the ellipsoidal particle. As the magnetic field strength increases to a large enough value, the particle could not perform a complete rotation and reaches a steady angle. With other different directions of the magnetic field, the period of rotation and asymmetry of the angular dynamics is also modified.

Keywords:

1. Introduction

Non-spherical microparticles are widely encountered in industrial, environmental and biological fluids: for example wood fibers in the paper-making industry[1], suspensions in complex fluids[2], and various micron-sized biological objects[3]. In biology and bioengineering, shape is one of the most important physical attributes of biological relevant particles[3,4]. It plays an important role in various applications of biomedicine and biology, such as diagnosis of diseases[5], drug delivery[6] and cell synchronization[7]. Because biological particles are often suspended in fluid environments, it is critical to understand the fundamental transport behaviors of non-spherical particles suspended in fluids. Over the last few decades there have been comprehensive theoretical and experimental investigations about the motion of ellipsoidal particle in a simple shear flow[8–11].

Jeffery[8] firstly studies the motion of ellipsoidal particle immersed in a simple shear viscous flow. The periodic motion of particle is so called "Jeffery orbits". The rotation period of a prolate spheroid with an aspect ratio *AR* (major semi-axis length / minor semi-axis length) in a simple shear flow **U** = ($\dot{\gamma}y$, 0, 0) is given by

$$T = \frac{2\pi}{\dot{\gamma}}\left(AR + \frac{1}{AR}\right). \quad (1)$$

The angle between the particle's major axis and the z-axis, θ, and the angle between the y-axis and xy-projection of the particle axis, ϕ, are shown in Figure 1, which are given by

$$tan\theta = \frac{C \cdot AR}{\sqrt{AR^2 cos^2\phi + sin^2\phi}}, \quad (2)$$

$$tan\phi = ARtan\left(2\pi\frac{t}{T}\right), \quad (3)$$

where C is the orbit constant determined by the initial orientation of the particle. For C=∞ (θ=90°), the particle just rotates in xy-plane, which means that ϕ only depends on the particle aspect ratio and the flow shear rate.

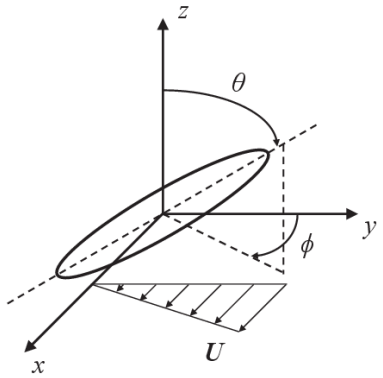

Figure 1. Schematic of an ellipsoidal particle in a simple shear flow

In this paper, a 2D fluid-structure interaction (FSI) model is created to study the effect of magnetic field and particle aspect ratio on the period of rotation and symmetry of ellipsoidal paramagnetic particles. The paper is organized as follows. In Section 2, the simulation method, including mathematical model, COMSOL setting and material properties, is presented. In Section 3, we first compare the rotational period obtained from the simulation to Jeffery's theory. Then we present the results and discussion about the effect of the strength and

direction of magnetic field and particle aspect ratio on particle. In Section 4, the main conclusions of this study are summarized.

2. Simulation method

2.1 Mathematical model

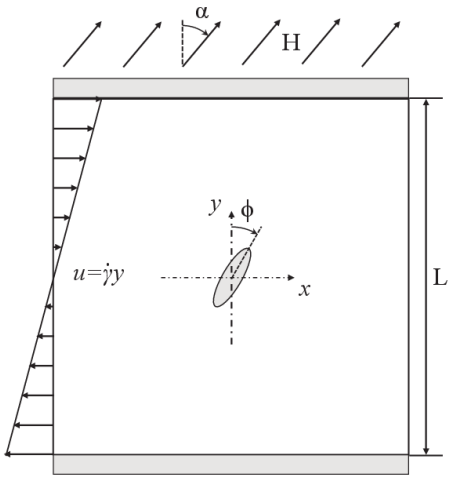

Figure 2. An ellipsoidal particle suspended in a simple shear flow and under a magnetic field **H**, which is directed at an angle α.

We consider an ellipsoidal particle immersed in a simple shear viscous flow in a Newtonian fluid with density ρ_f and dynamic viscosity η_f as shown in Figure 2. The center of the particle, coinciding with the origin of Cartesian coordinate system, is located in the center of a square computational domain. The particle aspect ratio is AR = a/b, where *a* and *b* are the major and minor semi-axis lengths of particles, respectively. The length of the computational domain is *L*. The rotation angle of particle is defined as ϕ between the major axis of the particle and *y* axis. The shear flow is u=$\dot{\gamma}y$, where $\dot{\gamma}$ is the shear rate of flow. A uniform magnetic field, **H,** is imposed at an arbitrary direction, denoted by α.

The Jeffery orbits are obtained with the assumption of Stokes flow, i.e., zero Reynolds number and no fluid inertia. Therefore, the flow field, $\boldsymbol{u}$, is governed by the continuity equation and Stokes equation:

$$\begin{aligned} \nabla \cdot \boldsymbol{u} &= 0, \\ \rho_f \frac{\partial \boldsymbol{u}}{\partial t} &= \nabla \cdot [-p\boldsymbol{I} + \eta_f(\nabla \boldsymbol{u} + (\nabla \boldsymbol{u})^T)], \end{aligned} \tag{4}$$

where *p* is the pressure.

To have a simple shear flow, the velocities of top and bottom walls are set to have the same magnitude but opposite directions. The periodic flow conditions are set to the left and right boundaries of the computational domain. No-slip condition is set on the particle surface, so the fluid velocities on the particle surface are given as:

$$\mathbf{u} = \mathbf{U}_p + \boldsymbol{\omega}_p \times (\mathbf{x}_s - \mathbf{x}_p), \tag{5}$$

where $\mathbf{U}_p$ and $\boldsymbol{\omega}_p$ are the translational and rotational velocities of particle, respectively. $\mathbf{x}_s$ and $\mathbf{x}_p$ are the position vectors of the surface and the center of the particle. The hydrodynamic force and torque acting on the particle are expressed as:

$$\mathbf{F}_{\mathrm{H}} = \int (\boldsymbol{\tau}_H \cdot \boldsymbol{n}) dS, \tag{6}$$

$$\mathbf{T}_{\mathrm{H}} = \int [\boldsymbol{\tau}_H \times (\mathbf{x}_s - \mathbf{x}_p) \cdot \boldsymbol{n}] dS, \tag{7}$$

where $\boldsymbol{\tau}_H = -p\boldsymbol{I} + \eta_f(\nabla \boldsymbol{u} + (\nabla \boldsymbol{u})^{\boldsymbol{T}})$ is the hydrodynamic stress tensor on the surface of particle.

The governing equations of the uniform magnetic field are given as:

$$\begin{aligned} \mathbf{H} &= -\nabla V_m, \\ \nabla \cdot \mathbf{H} &= 0, \end{aligned} \tag{8}$$

where V_m is the magnetic potential. The magnetic potential difference to generate the magnetic field is set on the top and bottom wall. Magnetic insulation boundary condition is applied on the left and the right boundaries of the computational domain.

Since the magnetic field is uniform, the force acting on the particle is zero. The magnetic torque acting on particle is expressed as[12]:

$$\mathbf{T}_{\mathrm{m}} = \mu_0 V_p(\chi_p - \chi_f)\boldsymbol{H}^{-} \times \boldsymbol{H}_0, \tag{9}$$

where $\boldsymbol{H}^{-}$and $\boldsymbol{H}_0$ are the magnetic fields inside and outside the particle, respectively. χ_p and χ_f are the magnetic susceptibilities of the particle and fluid, respectively. μ_0 is the permeability of vacuum, and V_p is the volume of particle.

The translation and rotation of particle are governed by Newton's second law:

$$m_p \frac{d\boldsymbol{U}_p}{dt} = \boldsymbol{F}_H, \tag{10}$$

$$I_p \frac{d\boldsymbol{\omega}_p}{dt} = \boldsymbol{T}_H + \boldsymbol{T}_m, \tag{11}$$

where m_p and I_p are the mass and the moment of inertia of the particle. The angular velocity of particle $\boldsymbol{\omega}_p = \boldsymbol{\omega}_h + \boldsymbol{\omega}_m$, where $\boldsymbol{\omega}_h$ is the angular velocity produced by hydrodynamic torque and $\boldsymbol{\omega}_m$ is the angular velocity produced by magnetic torque. At each time step, the position of center $\mathbf{C_p}(t) = (X_p, Y_p)$ and orientation $\phi_p(t) = \phi(t)$ of the particle are expressed as:

$$\boldsymbol{C}_{\boldsymbol{p}}(t) = \boldsymbol{C}_{\boldsymbol{p}}(0) + \int_0^t \boldsymbol{U}_p(s) ds, \tag{12}$$

$$\phi_p(t) = \phi_p(0) + \int_0^t \boldsymbol{\omega}_p(s) ds, \tag{13}$$

where $\boldsymbol{C}_{\boldsymbol{p}}(0)$ and $\phi_p(0)$ are the initial position and orientation of the particle.

2.2. COMOL settings

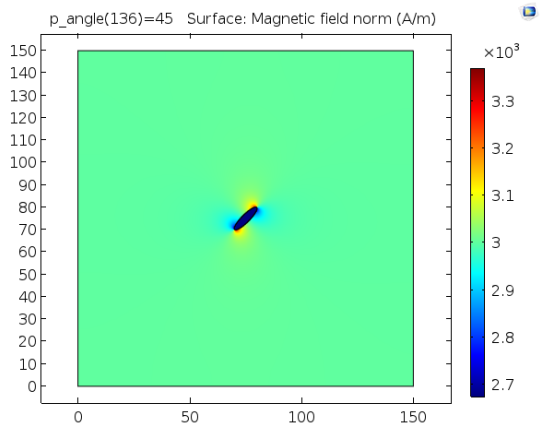

Figure 3. Magnetic field around the particle under the uniform magnetic field of H_0=3000A/m at ϕ=45°.

To calculate the magnetic torque acting on the particle, the magnetic field around the ellipsoidal particle is first computed by the AC/DC module in COMSOL Multiphysics® software. Figure 3 shows the magnetic field around the particle in the computational domain under the magnetic field of H_0=3000A/m, directed at α=0. Stationary Solver with Parametric Sweep analysis are used to calculate the magnetic field inside and outside of the particle at different rotation angle ϕ. Due to the symmetry of ellipsoidal particle, the simulation was conducted at ϕ from -90° to 90° with an angle step of 1°.

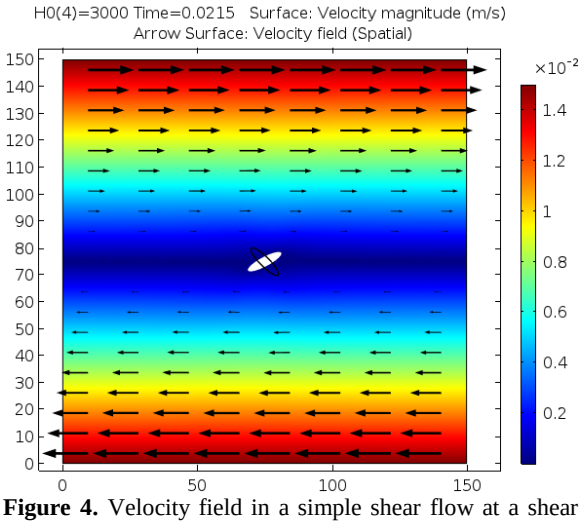

Figure 4. Velocity field in a simple shear flow at a shear rate of $\dot{\gamma}$=200 s^{-1}.

The fluid-structure interaction (FSI) model is solved by using the arbitrary Lagrangian-Eulerian (ALE) method. The detailed implementation of this method can be found in the paper of Hu et al[13]. Modelling of FSI is realized by combining Creeping Flow component in Fluid Flow module, Global ODEs and DAEs and Moving Mesh components in Mathematics module as shown in Figure 4.

Creeping Flow component is used to compute the flow field around the ellipsoidal particle. The top and bottom walls are set as moving wall condition with velocities at 1.5mm/s and -1.5mm/s respectively. Hence, the corresponding shear rate is 200 s^{-1}. The left and right boundaries are set as periodic flow conditions with zero pressure difference. No-slip boundary condition is set on the surface of particle, so the particle wall is set as a moving wall with fluid velocity of **u** as defined in Eq. (4).

The translational and rotational motion of the particle is determined by solving ordinary differential equations (ODEs) in Global ODEs and DAEs component. Eq. (10)-(13) are used in Global Equations to calculate translational and rotational velocities, and the position and orientation of the particle at each time step.

Moving Mesh component is used to describe the deforming mesh at the particle-fluid boundaries. Automatic Remeshing is enabled to re-initialize the mesh when the mesh quality below a threshold value, in this case, 0.2.

2.3 Material properties

In this study, the fluid and particles in the simulations are water and polystyrene particles respectively. The density and dynamic viscosity of water are 1000 kg/m^3 and 1.002×10^{-3} Pa·s respectively. The magnetic susceptibilities of fluid and particle are 0 and 0.26 respectively. The density of particle is 1100 kg/m^3. The particles used in the simulation have varying aspect ratios, but have the same volume, which is equivalent to a 7 μm-diameter sphere.

3. Results and Discussion

3.1. Validation of numerical method

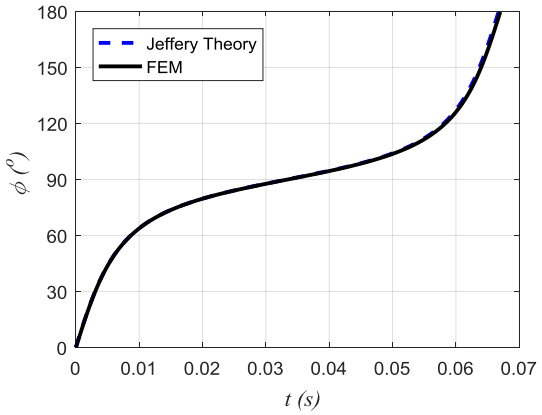

Figure 5. Comparison of the period between Jeffery's theory and the FEM simulation.

We first compare the results of our simulation to Jeffery's theory. Figure 5 shows the period of rotation of Jeffery's theory and our simulation for particle aspect ratio AR=4 without an applied magnetic field. The theoretical period of Jeffery orbit is 0.06675s; the period in this simulation is 0.0670s. The relative error is 0.37%, suggesting that this simulation has a remarkable agreement with the theory. Therefore, this simulation method has been validated to be sufficiently accurate to study the periodic rotation of particle immersed in the simple shear flow.

3.2. The effect of magnetic field strength

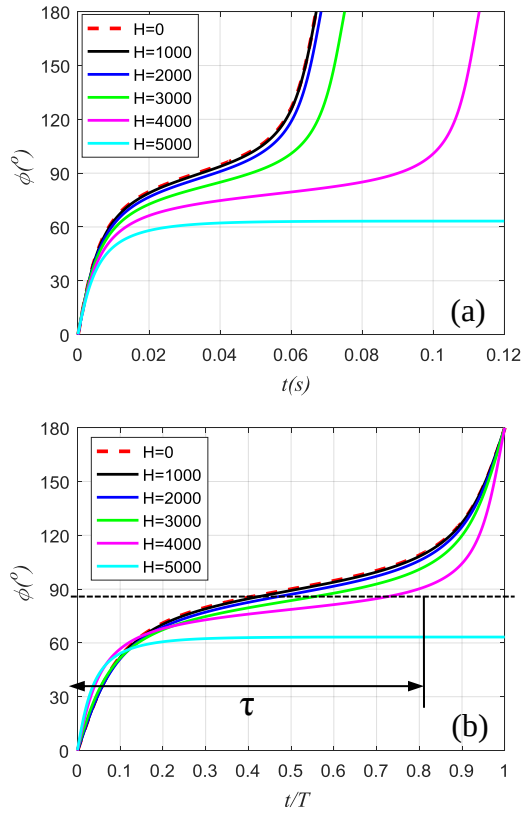

Figure 6. The effect of magnetic field strength H (A/m) on the rotation period and asymmetry of the particle rotation. The magnetic field is applied at angle strength (α=0°).

In this section, we investigate the effect of magnetic field strength on the period and asymmetry of rotation of particle for aspect ratio AR=4. Figure 6a shows that the angle of rotation, ϕ, corresponding to rotation time, t, with different magnetic field strength at the direction α=0°. It is shown that the rotation period increases with increasing magnetic field strength. Interestingly, as the magnetic field strength increases to a large enough value, the particle could not perform a complete rotation and reaches a steady angle. In this case, when the magnetic field strength is 5000A/m, the rotation angle stays at 63.28°. Figure 6b shows that that the angle of rotation, ϕ, corresponding to the dimensionless rotation time, t/T, with different magnetic field strength at the direction α=0°, where T is the rotation period obtained in Fig 6a. We defined a ratio parameter $\tau=T_1/T$ to characterize the symmetry and asymmetry of particle rotation as shown in Figure 6b, where T_1 is the time the particle rotating from ϕ=0° to ϕ=90°. So the time the particle rotation from ϕ=90° to ϕ=180°, $T_2=T-T_1$. When magnetic field strength is 0A/m, the curve is axisymmetric to (t/T, ϕ) = (0.5, 90°), where τ=0.5. It is consistent with Jeffery's theory. However, when magnetic field strength is 1000A/m, the symmetry is broken, and τ>0.5. As the magnetic field strength increases, τ become larger and larger, which means the asymmetry of rotation becomes more pronounced.

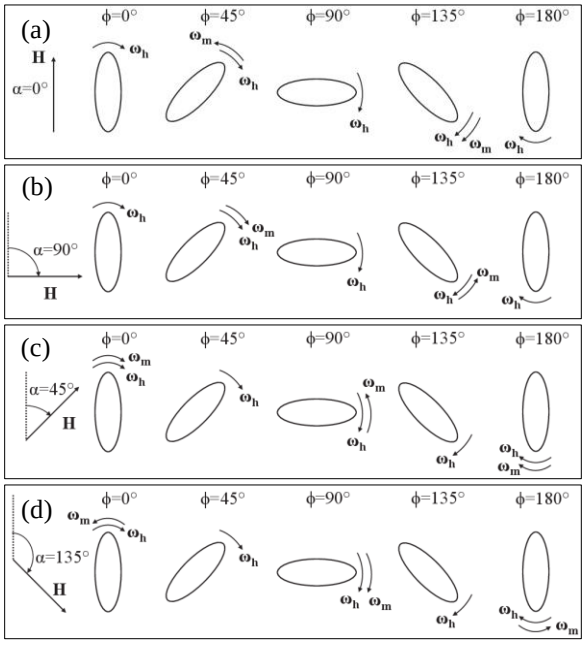

Figure 7. Illustration of particle rotation in the combined flow and magnetic fields.

The rotation behavior of the particle during one period in the combined flow and magnetic fields at α=0° is illustrated in Figure 7a. Without the magnetic field applied, only the hydrodynamic torque acts on the particle and rotates in the clockwise direction. When the magnetic field is applied at α=0°, the angular velocity produced by magnetic torque, $\boldsymbol{\omega}_m$, rotates in counterclockwise direction from ϕ=0° to ϕ=90°, which is the opposite to the angular velocity produced by hydrodynamic torque, $\boldsymbol{\omega}_h$; while $\boldsymbol{\omega}_m$ rotates in clockwise direction from ϕ=90° to ϕ=180°, which is the same as $\boldsymbol{\omega}_h$. Therefore, the particle will

rotate slower, and spend more time from ϕ=0° to ϕ=90°, while less time from ϕ=90° to ϕ=180°, that is, $T_1>T_2$. That is the reason why τ>0.5 when a magnetic field is applied. The larger the magnetic field strength, the larger τ. When the magnetic field strength increases to a large enough value, $\boldsymbol{\omega}_m$ will be equal to $\boldsymbol{\omega}_h$ in a certain angle between ϕ=0° and ϕ=90° and the particle will stop rotating. For magnetic field directed at other directions, the effect is illustrated in Fig 7b-d, and will be discussed further in the next section.

3.3. The effect of the direction of magnetic field

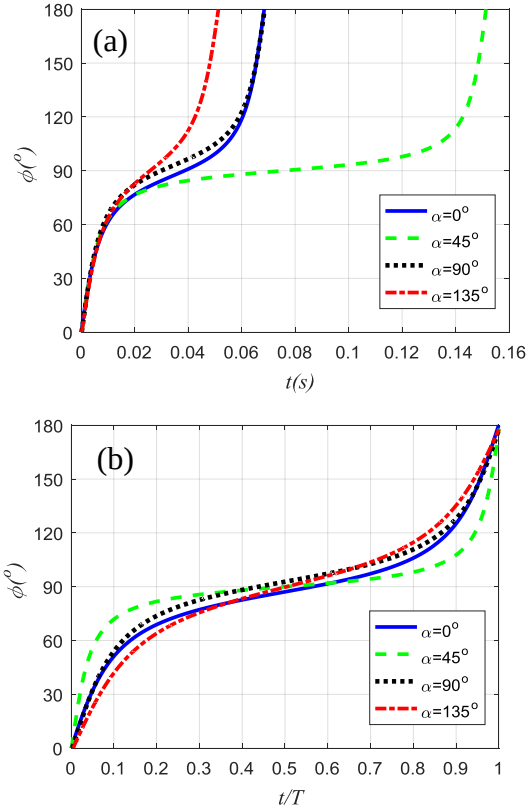

Figure 8. The effect of the direction of magnetic field at a fixed strength (H=2000A/m) on the rotational period and asymmetry of particle rotation.

In this section, the effect of the direction of magnetic field on the period and asymmetry of rotation of particle for aspect ratio AR=4 is investigated. Figure 8a shows that the angle of rotation corresponding to rotation time with different direction of magnetic field at strength H=2000A/m. The results show that the period of rotation at α=45° become longer than the period at α=0°, while the period of rotation at α=135° become shorter than the period at α=0°. The periods of rotation are almost the same at α=90° and α=0°. The angle of rotation corresponding to the dimensionless time with different direction of magnetic field at strength H=2000A/m is shown in Figure 8b. As we can see, τ > 0.5 when α=0°, while τ < 0.5 when α=90°. τ = 0.5 when α=45° and 135°. The rotation behaviors of one period in the combined flow and magnetic fields at the different direction are shown in Figure 7. As we discussed before, the particle spend more time from ϕ=0° to ϕ=90°, while less time from ϕ=90° to ϕ=180° at α=0°. For α=90°, $\boldsymbol{\omega}_m$ and $\boldsymbol{\omega}_h$ have the same direction from ϕ=0° to ϕ=90°, while have the opposite direction from ϕ=90° to ϕ=180° shown in Figure 7b. It means that the particle spends less time from ϕ=0° to ϕ=90°, while more time from ϕ=90° to ϕ=180° at α=0°, that is, $T_1<T_2$ and τ < 0.5. For α=45°,$\boldsymbol{\omega}_m$ and $\boldsymbol{\omega}_h$ have the same direction from ϕ=0° to ϕ=45° and ϕ=135° to ϕ=180°, while have the opposite direction from ϕ=45° to ϕ=135° shown in Figure 7c. Due the symmetry of flow field and particle, the time spending from ϕ=0° to ϕ=45° and ϕ=135° to ϕ=180° are equal. At the same time, the time spending from ϕ=45° to ϕ=90° and ϕ=90° to ϕ=135° are equal. So $T_1=T_2$ and τ =0.5. The similar reason can explain the rotation behavior at α=135° shown in Figure 7d.

3.4. The effect of particle aspect ratio

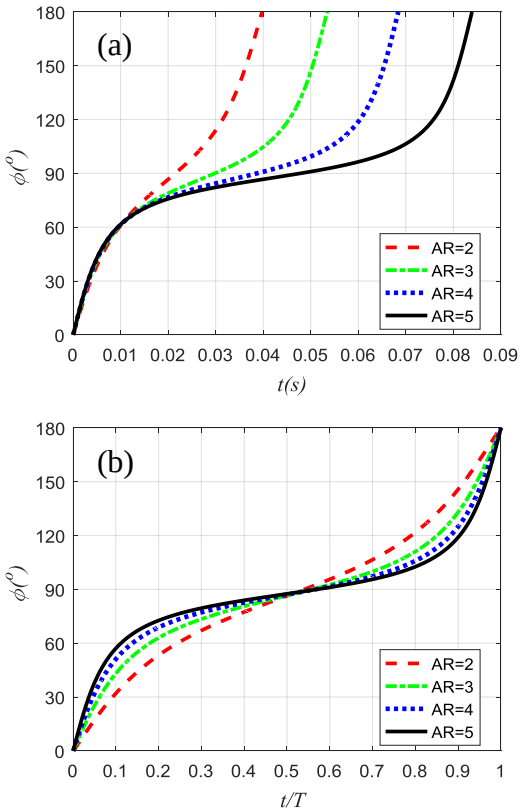

Figure 9. The effect of particle aspect ratio on the rotational period and asymmetry of particle rotation at (H=2000A/m, α=0°).

In this section, we study the effect of particle aspect ratio on the period and asymmetry of rotation of particle. Figure 9a shows that the angle of rotation corresponding to rotation time with different particle aspect ratio at H=2000A/m and α=0°. As particle aspect ratio increases, the period of rotation increases, agreeing well with the trend predicted by Jeffery's theory. Figure 9b shows the angle of rotation corresponding to the dimensionless time with different particle aspect ratio at H=2000A/m and α=0°. It is shown that τ is always larger than 0.5 for different particle aspect ratio, which is consistent with what we discussed before. When aspect ratio increases, there is a slight increase for τ, which means that particle aspect ratio has only a marginal effect on the asymmetry of rotation of particle.

4. Conclusions

The motion of ellipsoidal particles in a simple shear flow subjected to a uniform magnetic field is numerically investigated by a multiphysics model that couples magnetic field, flow field and rigid body motions. The magnetic field strength has a significant effect on the period and asymmetry of rotation of particle. As the magnetic field strength increases, the rotation period of particle increases and the asymmetry of rotation becomes more pronounced. When the magnetic field strength increases to a large enough value, the particle could not perform a complete rotation and reaches a steady angle. Further, the direction of magnetic field modifies both the period and asymmetry of rotation of particle. Placed at 45°, the direction of magnetic field shortens the period of rotation, while at 135° it increases the period. The symmetry of particle rotation is preserved for magnetic fields placed at 45° and 135°. The magnetic field, when directed at 0° and 90°, causes the asymmetry of rotation. For particle aspect ratio, the results show that it changes the period of rotation of particle, which is consistent with Jeffery's theory, but has a subtle effect on the asymmetry of particle rotation.

References

1. Alava M, Niskanen K. The physics of paper. *Reports on Progress in Physics* 2006; **69**(3):669–723.
2. Ronald G Larson. *The structure and rheology of complex fluids*. New York : Oxford University Press; 1999.
3. Young KD. The selective value of bacterial shape. *Microbiology and molecular biology reviews : MMBR* 2006; **70**(3):660–703.
4. Mitragotri S, Lahann J. Physical approaches to biomaterial design. *Nature materials* 2009; **8**(1):15–23.
5. Anstey NM, Russell B, Yeo TW, Price RN. The pathophysiology of vivax malaria. *Trends in Parasitology* 2009; **25**(5):220–227.
6. Champion JA, Katare YK, Mitragotri S. Particle shape: A new design parameter for micro- and nanoscale drug delivery carriers. *Journal of Controlled Release* 2007; **121**(1–2):3–9.
7. Valero A, Braschler T, Rauch A, Demierre N, Barral Y, Renaud P. Tracking and synchronization of the yeast cell cycle using dielectrophoretic opacity. *Lab on a chip* 2011; **11**(10):1754–1760.
8. Jeffery GB. The Motion of Ellipsoidal Particles Immersed in a Viscous Fluid. *Proceedings of the Royal Society A: Mathematical, Physical and Engineering Sciences* 1922; **102**(715):161–179.
9. Taylor GI. The Motion of Ellipsoidal Particles in a Viscous Fluid. *Proceedings of the Royal Society of London. Series A, Containing Papers of a Mathematical and Physical Character* 1923; **103**:58–61.
10. Saffman PG. On the motion of small spheroidal particles in a viscous liquid. *Journal of Fluid Mechanics* 1956; **1**(5):540–553.
11. Leal LG. Particle Motions in a Viscous-Fluid. *Annual Review of Fluid Mechanics* 1980; **12**:435–476.
12. Stratton JA, Press I, Wiley AJ. *Electromagnetic Theory By*.; 2007.
13. Hu HH, Patankar N a., Zhu MY. Direct Numerical Simulations of Fluid–Solid Systems Using the Arbitrary Lagrangian–Eulerian Technique. *Journal of Computational Physics* 2001; **169**:427–462.

Acknowledgements

The authors gratefully acknowledge the financial support from the Department of Mechanical and Aerospace Engineering at Missouri University of Science and Technology.